Agricultural and Forest Meteorology 221 (2016) 142–151

Contents lists available at ScienceDirect

Agricultural and Forest Meteorology

journal homepage: www.elsevier.com/locate/agrformet

Seasonal variation in ecosystem water use efficiency in an urban-forest reserve affected by periodic drought

Jing Xie[a,b,c], Tianshan Zha[a,b,*], Caixian Zhou[c], Xin Jia[a,b,d], Haiqun Yu[c], Bai Yang[e], Jiquan Chen[f], Feng Zhang[c], Ben Wang[a,b,d], Charles P.-A. Bourque[g], Ge Sun[h], Hong Ma[c], He Liu[i], Heli Peltola[d]

[a] College of Soil and Water Conservation, Beijing Forestry University, Beijing 100083, PR China
[b] Key Laboratory of Soil and Water Conservation and Desertification Combating, Ministry of Education, Beijing Forestry University, Beijing 100083, China
[c] Beijing Forestry Carbon Sequestration Administration, Beijing, 100013, PR China
[d] School of Forest Sciences, University of Eastern Finland, PO Box 111, FIN-80101 Joensuu, Finland
[e] Environmental Sciences Divisions, Oak Ridge National Laboratory, Oak Ridge, TN 37831, USA
[f] CGCEO/Geography, Michigan State University, East Lansing, MI 48823, USA
[g] Faculty of Forestry and Environmental Management, University of New Brunswick, PO Box 4400, Fredericton, New Brunswick E3B 5A3, Canada
[h] Eastern Forest Environmental Threat Assessment Center, Southern Research Station, USDA Forest Service, Raleigh, NC 27606, USA
[i] Beijing Forestry University, Beijing 100083, PR China

ARTICLE INFO

Article history:
Received 30 August 2015
Received in revised form 11 February 2016
Accepted 14 February 2016
Available online 26 February 2016

Keywords:
Climate warming
Eddy covariance
Evapotranspiration
Extreme drought
Gross ecosystem production

ABSTRACT

The impact of extreme weather events on water-carbon coupling and ecosystem water use efficiency (WUE) in arid to semi-arid conditions is poorly understood. Evapotranspiration (ET) and gross ecosystem production (GEP) were based on continuously eddy-covariance measurements taken over an urban-forest reserve in Beijing, in a 3-year period (2012–2014) to calculate WUE (GEP:ET). Our objective was to investigate the seasonal response of WUE to changing environmental and drought conditions at different timescales. Annually, the forest produced new plant biomass at 2.6 ± 0.2 g C per kg of water loss. Within each season, interactions of surface conductance (g_c) and normalized difference vegetation index (NDVI; *i.e.*, $g_c \times$ NDVI) in spring, net radiation (R_n) and air temperature (T_a; *i.e.*, $R_n \times T_a$) in summer, and R_n and vapor pressure deficit (D; *i.e.*, $R_n \times D$) in autumn were found as the significant variables explaining seasonal variation in WUE. Daily WUE correlated positively with T_a and NDVI during the growing season, but a negative relationship during excessively dry periods (*i.e.*, 2014). Daily WUE decreased during warm and dry days or remained nearly constant at low levels due to proportional decreases in GEP and ET. An extreme drought during the leaf expansion led to a greater decline in GEP than in ET, causing WUE to be lower in 2012 and 2014 than that in 2013. In contrast, an extreme drought during the leaf coloration led to a greater decline in ET than in GEP, causing higher WUE in 2013 and 2014 than that in 2012. We concluded that: (i) high soil water content (SWC) during leaf expansion was more important than high SWC in mid-summer or autumn for maintaining a high seasonal WUE; and that (ii) seasonal water availability combined with variable drought severity and duration during periods of changing T_a, caused seasonal ET and GEP to respond differently, introducing significant variation in seasonal WUE.

1. Introduction

Afforestation in China has been increasing since 1949, with levels of afforested areas expanding every year (Gao et al., 2014). As a consequence of global warming, local shortages of available water have been documented to occur more frequently, and its devastating impact is increasingly becoming apparent in Northeastern China (Zhai et al., 2010). Extreme warm and dry conditions of protected environments may locally counteract the positive effects of atmospheric CO_2 enrichment and plant fertilization, causing gross ecosystem production (GEP) and, thus, ecosystem water use efficiency (WUE) to decline (Huang et al., 2015). However, little is known about how ecosystem-level WUE of forest plantations respond to climate warming and extreme drought over extended

* Corresponding author at: College of Soil and Water Conservation, Beijing Forestry University, Beijing 100083, PR China.
E-mail addresses: tianshanzha@bjfu.edu.cn, ts_zha@hotmail.com (T. Zha).

http://dx.doi.org/10.1016/j.agrformet.2016.02.013
0168-1923/

periods (*e.g.*, several years) due to the complexity of ecosystem response behaviors.

Ecosystem WUE is considerably important in the investigation of forest carbon (C) assimilation relative to water vapor loss by evapotranspiration (ET; Kuglitsch et al., 2008; Yang et al., 2010). Ecosystem-level assessment of WUE is effective at determining the adaptability of protected urban-forest plantations to variable climate (Beer et al., 2009; Xie et al., 2014). Current thinking about ecosystem-WUE responses to incidences of warming and drying conditions, or extreme climate events, is mixed throughout the scientific literatures. For example, modeling studies suggest that ecosystem WUE may decrease under conditions of climate warming (De Boeck et al., 2006; Bell et al., 2010; Niu et al., 2011). Consistent with this view, Reichstein et al. (2007) detected a slight decrease in WUE for European forests during a severe heatwave in the summer of 2003. Also, Ponton et al. (2006), Tang et al. (2006), and Kuglitsch et al. (2008) found WUE to be lower when precipitation was low. In contrast, Ponce-Campos et al. (2013) and Xiao et al. (2013) found that WUE tended to increase when air temperature (T_a) was high. Krishnan et al. (2006), Li et al. (2008), Yu et al. (2008), and Beer et al. (2009) reported similar increases in WUE during periods of excessive dryness.

Literature dissensus stems, in part, from: (i) the different ways in which data were acquired (*e.g.*, stratified or non-stratified) and processed and/or the different timescales of integration (*e.g.*, hourly, daily, or annual timescales; Yang et al., 2010); (ii) water losses from the canopy and soil surface (*i.e.*, ET) are theorized to have different sensitivities to changes in T_a and precipitation (Ponton et al., 2006; Hu et al., 2008; Niu et al., 2011); and (iii) lack of consensus as to atmosphere-plant exchanges of C and water vapor under different environmental conditions. For example, Law et al. (2002), Ponton et al. (2006), and Yu et al. (2008) found that increases in ET occurred faster than increases in GEP under increasing T_a. Zhang et al. (2014) reported an opposite trend, which is largely explained by the positive effects of optimum temperature on plant photosynthesis.

Previous studies have shown that WUE is controlled by the interactions between the number of sites and biophysical variables (Kuglitsch et al., 2008). However, information about these controls, especially for protected urban forests during extreme environmental conditions, is lacking. Although the role of environmental variables in regulating ecosystem WUE in urban forests is complicated and challenging to investigate, improved understanding of ecosystem WUE is clearly central to assessing acclimatization of urban forests to extreme dry conditions, as reductions in regional precipitation intensify with climate change. Given the ongoing, extreme changes in the climate system, attaining a mechanistic understanding of the long-term dynamics of ecosystem WUE, including identification of its key controlling variables, is an important research objective.

In this study, we measured water vapor and C fluxes over a manmade nature reserve in Beijing, China (*i.e.*, Beijing Olympic Forest Park) during a three-year period (2012–2014). Flux measurements were acquired with the eddy covariance (EC) technique. This technique provides direct measurements of water vapor and C exchanges between forests and the atmosphere, providing a basis in examining forest WUE at the ecosystem level (Falge et al., 2001; Zha et al., 2013). The measurement period covers events with extreme annual total precipitation levels (from extremely low to very high) and annual mean T_a (high), compared to the past 50 years. The particular objectives of this study were to: (i) determine the environmental variables affecting ecosystem WUE in an urban forest over several timescales, and (ii) examine the seasonal response of WUE to climate extremes, particularly drought, common to Northeastern China.

2. Materials and methods

2.1. Study site

The study site is located in Beijing Olympic Forest Park (40.02°N, 116.38°E), Beijing, China. It is the largest manmade urban-forest park in Asia, with an area of 680 ha and vegetation coverage of about 90%. The forest-reserve is located in the middle of the northeastern section of the park, an area committed to ecological conservation and recovery. Tourists are restricted from entering the study area and recreational facilities are minimized in order to reduce human disturbance.

The area is classified as having a continental, semi-humid monsoon climate, with a mean annual T_a of 12.5 °C and frost-free period of about 190 days. Mean annual total precipitation is 592 mm, of which 80% falls between June and August. The soil is mainly of the fluvo-aquic type, with soil porosity of 40.3%, pH of 7.8, and an estimated field capacity and permanent wilting point of 26% and 10%, respectively. Historical climate data are from the Chaoyang District meteorological station nearby, and are summarized as averages over a 50-year period (1961–2010).

The flux site is characterized by flat topography with slopes <5° and elevations of 51 m above sea level (a.s.l.). Plant species composition and stand biometric properties were measured in a 1-ha permanent sampling plot. The young urban-plantation forest consisted of several tree species, with a shallow rooting depth of 0.08–0.40 m and mean age of 20 years, based on the age of overstory trees. The site is dominated by *Pinus tabulaeformis*; other species include *Platycladus orientalis*, *Sophora japonica* L., *Fraxinus chinensis*, and *Ginkgo biloba*, with an understory of *Iris tectorum* and *Dianthus chinensis*. All trees were tagged and identified by species, with diameter at breast height (DBH) >3 cm being assessed annually. Stand density in 2013 was 210 trees ha^{-1}, with a mean tree height of 7.7 m and a mean DBH of 0.2 m. Cover ratio of trees to shrubs was about 7:3. The shrubs included *Prunus davidiana*, *Amygdalus triloba*, *Swida alba*, and *Syzygium aromaticum*, with a mean height of 2.8 m. The growing season is defined as the period between the first and last occurrence of three consecutive days, when GEP is <5% of the summer maximum C uptake. We defined March through May as spring, June through August as summer, and September through November as autumn. Normally, tree leaf expansion and coloration stages begin in April and October, respectively. We defined duration and severity of 'drought' according to mean SWC <12.5% from spring to autumn; dry-soil periods during each year, are identified in Fig. 1a.

2.2. Flux, meteorological, and vegetation measurements

A 12-m-tall tower is surrounded by uniform forest cover with a homogeneous fetch of about 600 m in all directions. Carbon dioxide (CO_2) and water vapor (H_2O) exchanges are based on high-frequency measurements (at 10 Hz) obtained with EC equipment placed at the top of the tower (11.5-m height from ground). The EC system consists of a closed-path infrared gas analyzer [IRGA; model EC-155, Campbell Scientific, Inc. (CSI), Logan, UT, USA] and a sonic anemometer (CSAT3; CSI). The IRGA is calibrated quarterly using 99.99% nitrogen gas (zero offset calibration) and a standard CO_2 concentration of 650 ppm and a dew point generator (LI-610, LI-COR Inc., USA). Continuous data were collected and processed to calculate the corresponding fluxes at 30-min. intervals following the method described in Massman and Lee (2002). Sonic temperature was corrected for changes in atmospheric humidity and pressure (Schotanus et al., 1983). Net ecosystem CO_2 exchange (or negative net ecosystem production, NEP, μmol CO_2 m^{-2} s^{-1}) was calculated as the sum of the corrected CO_2 flux and the CO_2-storage change in the canopy-air layer. We adopted the sign convention

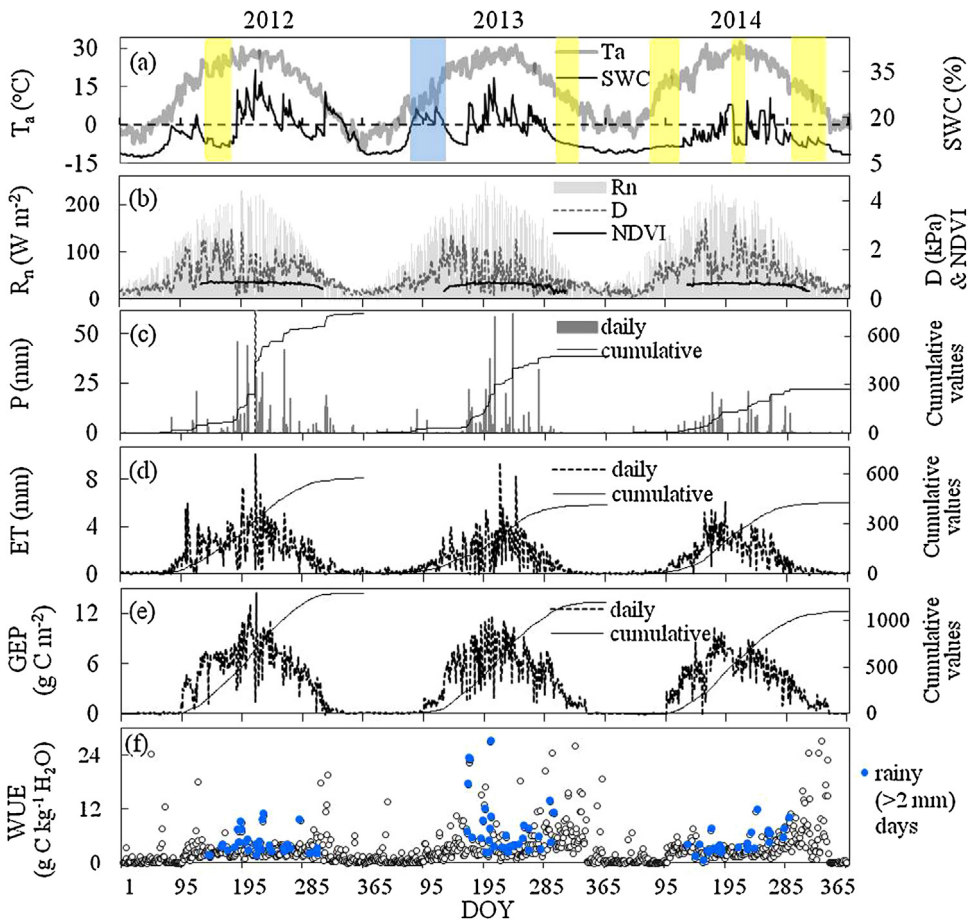

Fig. 1. Daily mean (a) air temperature (T_a), soil water content (SWC), (b) net radiation (R_n), vapor pressure deficit (D), normalized difference vegetation index (NDVI), (c) daily total precipitation (P), (d) evapotranspiration (ET), (e) gross ecosystem production (GEP), and (f) daily mean water use efficiency (WUE) from 2012 through 2014. Blue symbols in panel (f) signify rainfall events (with >2 mm) during May through to October. Yellow and blue shaded bands in plot (a) indicate periods of drought and wetness, respectively. One precipitation point (*i.e.*, 176 mm on DOY 203, 2012) in plot (c) is not shown.

that positive NEP denotes CO_2 fluxes moving toward the surface, associated with CO_2 uptake by plants.

Latent heat and sensible heat fluxes ($W\,m^{-2}$) are also derived from EC data. Above-canopy meteorological variables were measured at the top of the tower and also reported as 30-min means, including relative humidity (RH, %) and T_a (°C) with HMP-45C sensors (Vaisala, Helsinki, Finland), photosynthetically active radiation (PAR, $\mu mol\,m^{-2}\,s^{-1}$) with PAR-LITE sensors (Kipp and Zonen, Delft, the Netherlands), and net radiation (R_n, $W\,m^{-2}$) with a CNR-4 sensor (Kipp and Zonen, Delft, the Netherlands). Normalized difference vegetation index (NDVI) was calculated after Hmimina et al. (2013). Precipitation (mm) was recorded with a tipping bucket rain gauge (TE-525 MM, CSI) set at 0.7-m above the ground surface. Soil heat fluxes (G, $W\,m^{-2}$) were measured at four locations with HFP-01 flux plates (CSI) buried 10-cm below ground. Soil temperatures (T_s, °C) were monitored at four locations with CS-109 probes (CSI) placed at a 10-cm depth below ground. Volumetric soil water content (SWC, %) within the top 10-cm of the soil was measured at four locations using horizontally inserted CS-616 time domain reflectometers (CSI).

2.3. Data quality control and gap-filling

Eddy covariance data were screened for quality by flagging periods of highly stable or unstable atmospheric conditions, non-stationary turbulent fluxes, weather influence (*e.g.*, rain, dew, or ice on sensors), low turbulence, out-of-range fluxes, and power failures (Acevedo et al., 2009). All 30-min fluxes were checked for quality and consistency (Noormets et al., 2007), including stationarity, integral turbulence characteristics, and friction velocity (u^*) thresholds. The threshold of u^* below which flux loss occurred was determined from the seasonal binned relationships between nighttime turbulent fluxes of CO_2 and u^* (Schmid et al., 2000). Nighttime NEP-data were excluded, whenever corresponding u^*'s were <0.15 in 2012, 0.20 in 2013, and 0.18 $m\,s^{-1}$ in 2014. Data gaps accounted for 4%, 6%, and 5% of daytime and 28%, 31%, and 27% of nighttime NEP in 2012, 2013, and 2014, respectively. Mean percentage of gaps in NEP formed <35% of the total data reported in other studies (Xie et al., 2015; Falge et al., 2001).

A gap-filling model was chosen among evaluated model variants, based on magnitude and bias of residuals and stability of model-parameter estimates (Noormets et al., 2007). Uncertainty in annual NEP, which were caused by gaps in the data and the gap-filling model, were estimated according to the method described in Flanagan and Johnson (2005). Uncertainty in annual estimates of NEP (237 ± 26, $g\,C\,m^{-2}$), GEP (1195 ± 58, $g\,C\,m^{-2}$), and ecosystem respiration (ER; 958 ± 70, $g\,C\,m^{-2}$) were all within reported ranges (Baldocchi and Meyers, 1998; Falge et al., 2001; Xiao et al., 2013).

Different treatments were applied to daytime and nighttime gaps in CO_2 datasets. Specifically, gaps during the nighttime (PAR <3 $\mu mol\,m^{-2}\,s^{-1}$) were filled according to the relationship between ER and T_s [*i.e.*, Eq. (1); Zha et al., 2007], whereas those during the daytime (PAR ≥3 $\mu mol\,m^{-2}\,s^{-1}$) were filled on the basis of the relationship between daytime NEP, PAR, and ER [*i.e.*, Eqs. (1)

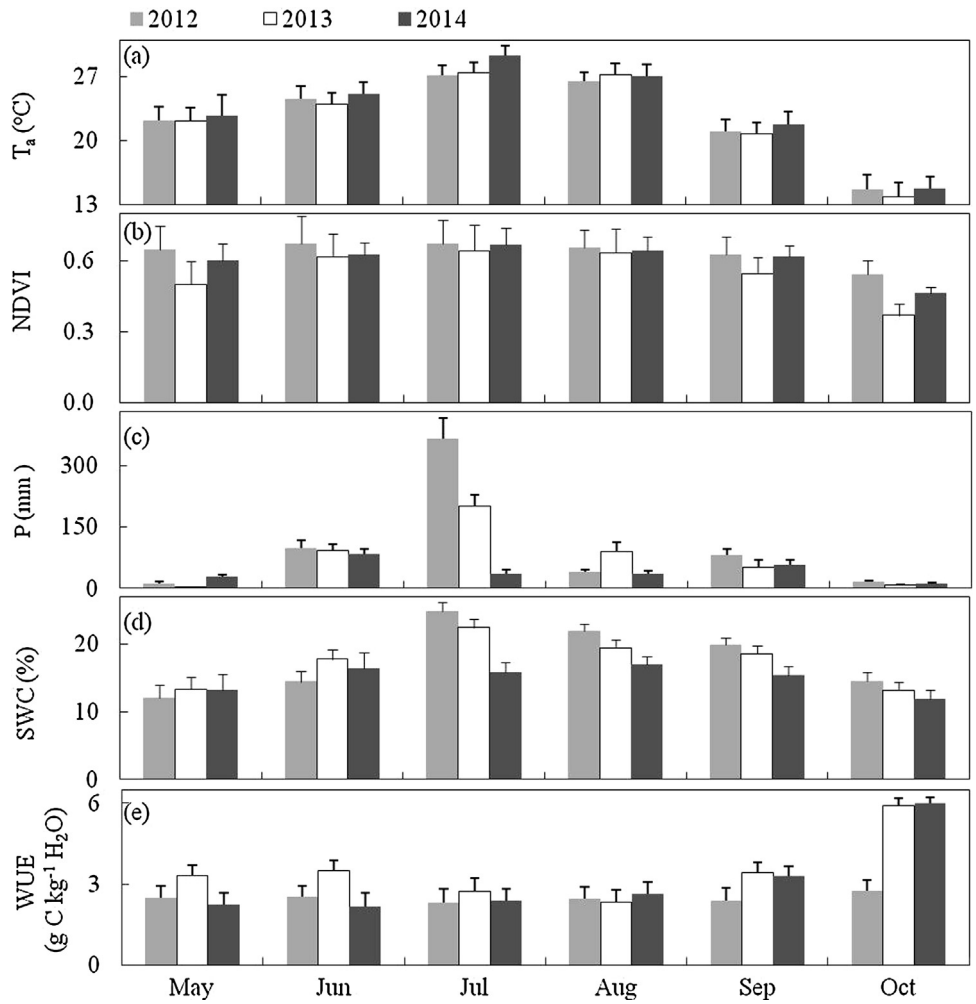

Fig. 2. Monthly values of (a) T_a, (b) NDVI, (c) total precipitation (P), (d) SWC, and (e) WUE from May to October 2012–2014.

and (2), below]. After 30-min estimates of ER were calculated with Eq. (1), gross ecosystem production (GEP) was calculated as the sum of NEP and ER (*i.e.*, GEP = NEP + ER). Each 30-min gap in NEP was filled using a dynamic parameter-setting procedure described by Noormets et al. (2007). The approach is based on a Lloyd–Taylor type equation (Lloyd & Taylor, 1994). The ER model was parameterized using nighttime data:

$$ER = R_0 \times Q_{10}^{(T_s/10)} \quad (1)$$

where R_0 is the nighttime ER-rate when T_s is at 0 °C, Q_{10} is a temperature coefficient of respiration (*i.e.*, the factor by which respiration increases with a 10 °C rise in T_s), and T_s is the soil temperature at a 10-cm depth (°C).Eq. (1) was established on a monthly scale before it was applied to estimate daytime ER, assuming there was consistent temperature sensitivity between nighttime and daytime exchanges. After daytime estimates of ER were generated, daytime NEP were filled with:

$$NEP = \frac{\alpha \times PAR \times P_{max}}{\alpha \times PAR + P_{max}} - ER \quad (2)$$

where PAR is photosynthetically active radiation (μmol m^{-2} s^{-1}), P_{max} is the maximum apparent photosynthetic capacity of the canopy (μmol CO_2 m^{-2} s^{-1}), and α is the apparent quantum yield (μmol CO_2 μmol^{-1} PAR). The first term to the right-hand-side of Eq. (2) provides a calculation of GEP.

Gaps in precipitation were replaced by precipitation records from the Chaoyang District meteorological station. Vapor pressure deficit (D, kPa) was calculated from the gap-filled T_a and RH records above the canopy. Other 30-min gaps of <1.5 h in meteorological variables with underlying diurnal cycles, were filled by linear interpolation, and longer gaps (*i.e.*, gaps ≥ 1.5 h) were filled with the Mean Diurnal Variation method of Falge et al. (2001).

2.4. Ecosystem WUE

Ecosystem WUE is defined here according to the definition used by ecologists—ratio of GEP to ET. Although ecosystem WUE can be expressed in other ways (*e.g.*, NEP:ET), GEP:ET is most commonly used (Law et al., 2002; Ponton et al., 2006; Kuglitsch et al., 2008; Yu et al., 2008; Niu et al., 2011; Huang et al., 2015). Extent of ET was estimated from measurements of latent heat flux, accounting for water vapor losses by plant transpiration (*i.e.*, dry-canopy transpiration) and evaporation from soil and plant surfaces (*i.e.*, canopy interception or wet-canopy evaporation). Park management activities, such as irrigation and other practices, which were not permitted within the fenced-area of the study site, should not hinder our interpretation of ET and WUE. Water use efficiency was calculated on various timescales. Daily GEP and ET were derived by summing their respective daytime daily values (PAR ≥ 3 μmol m^{-2} s^{-1}; Zha et al., 2007). Daily, seasonal, and annual WUE were quantified by daily, seasonal, and annual ratios of GEP:ET.

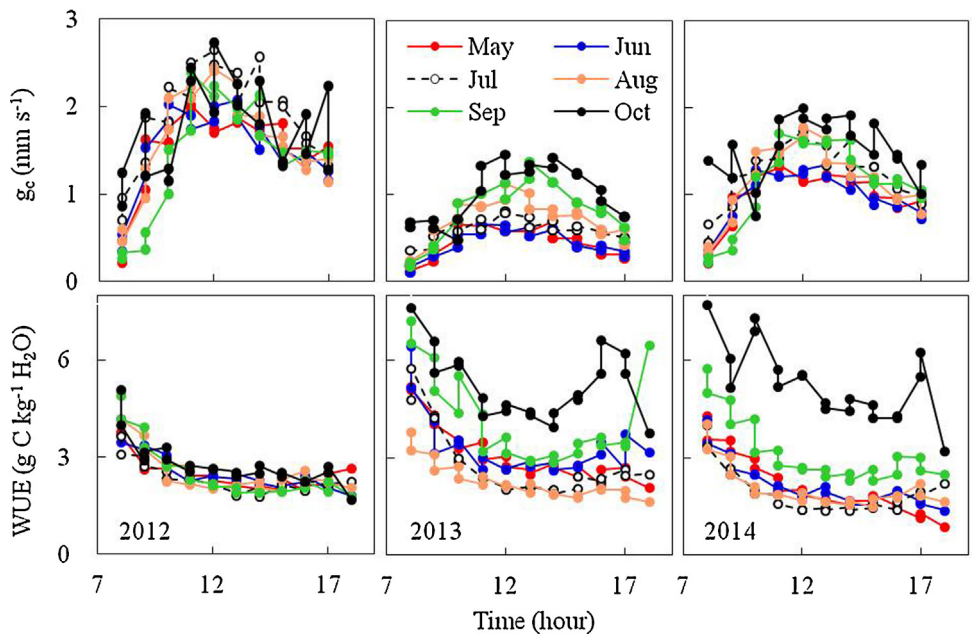

Fig. 3. Mean diurnal cycle of instantaneous surface conductance (g_c, mm s^{-1}) and water use efficiency (WUE, g C kg^{-1} H_2O) during the growing season (May–October) from 2012 to 2014 ($p < 0.05$).

2.5. Surface conductance

Instantaneous surface conductance (g_c, mm s^{-1}; Yoshida et al., 2010; Zha et al., 2013) was calculated by inverting the Penman–Monteith equation, giving

$$g_c = \frac{\lambda E \gamma g_a}{\Delta R_a + \rho_a C_p g_a D - \lambda E(\Delta + \gamma)} \quad (3),$$

where λ is the latent heat of vaporization (J kg^{-1}), E is measured ET in kg m^{-2} s^{-1}, γ (kPa °C^{-1}) is the psychrometric constant modified to account for variation in canopy and atmospheric resistances, Δ (kPa °C^{-1}) is the slope of the saturation water vapor pressure *vs.* temperature curve, ρa is the density of dry air (kg m^{-3}), and C_p is the specific heat of air at constant pressure (J kg^{-1} K^{-1}). Aerodynamic conductance, g_a (m s^{-1}), was calculated from u^* and wind speed above the canopy, which was measured with the sonic anemometer. Available energy, R_a (W m^{-2}), was calculated as the difference of net radiation (R_n), total energy storage in the forest-air column (S_t), and the soil heat flux (G), *i.e.*, $R_a = R_n - S_t - G$.

2.6. Statistical analysis

Linear and logarithmic regressions were used to examine the relationships between WUE and selected biophysical and environmental variables (*i.e.*, NDVI, g_c, T_a, R_n, D, SWC, and precipitation) at various timescales. We used Pearson's correlation coefficient (*PCC*) to describe associated linear relationships. All data processing and statistical analyses were conducted using the Statistical Analysis System v. 9.2 for Windows software (SAS, Institute, Inc., Cary, NC, USA).

3. Results

3.1. Microclimate

Annual mean T_a above the canopy increased over the three years, with the lowest annual value appearing in 2012 and the highest in 2014 (Table 1). All three years were warmer than the 50-year (1961–2010) average of 12.5 °C. Daily and monthly T_a and NDVI were highest in July or August (Figs. 1 a, b, 2 a, b). Over the three years, the highest daily mean R_n and D occurred in May, June, or July (Fig. 1b).

Although annual total precipitation in 2012 was 146 mm higher than the 50-year average, 2012 was noted for its many irregular and intensive precipitation events, compared to 2013 or 2014. For example, 24% of the annual total precipitation in 2012 fell during a single summer rain event (*i.e.*, 176 mm on DOY 203, dashed vertical line in Fig. 1c), yielding the greatest daily total precipitation in the last 50 years. In contrast, annual total precipitation in 2013 and 2014 were well below the 50-year average, especially with 2014 being short of about 321 mm from the long-term average. Daily precipitation events in 2013 were generally moderate in nature, whereas 2014 had few rainfall events (Fig. 1c). Annualized ratios of ET-to-precipitation (*i.e.*, evaporation effectiveness) increased during the three years, with ratios of 0.8 in 2012, 0.9 in 2013, and 1.6 in 2014.

Summer SWC in 2012 and 2013 were about the same, with seasonal means of 20.4% and 19.9%, respectively (Fig. 1a). Although annual precipitation was highest in 2012, soils in spring were generally drier in 2012 than in 2013, with seasonal SWC of 13.6% in 2012 and 16.9% in 2013 (Fig. 1a). Moderately high spring SWC in 2013 was mainly a result of high autumnal precipitation (168 mm) during the preceding year (*i.e.*, 2012; Fig. 1a, c).

Years 2012 and 2013 were both dry years, but not as dry as 2014. According to the number of consecutive low SWC days during the growing season, 2012 had one extreme dry-soil period (DOY 140–155) in spring, with a mean SWC of 11.2% (Fig. 1a). Year 2013 had one extreme dry-soil period (DOY 303–334) during the leaf-coloration period, with mean SWC of 10.9% (Fig. 1a). Year 2014 had the lowest annual and seasonal SWC (Table 1), with three extreme dry-soil periods (DOY 67–117, 191–228, and 289–334) during leaf-expansion, summer, and leaf-coloration periods, with mean SWC of 10.6%, 12.3%, and 10.8%, respectively (Fig. 1a).

3.2. Variation in water, carbon fluxes, and WUE

Highest annual ET and GEP both occurred in 2012, coinciding with the highest growing-season NDVI and longest growing-season

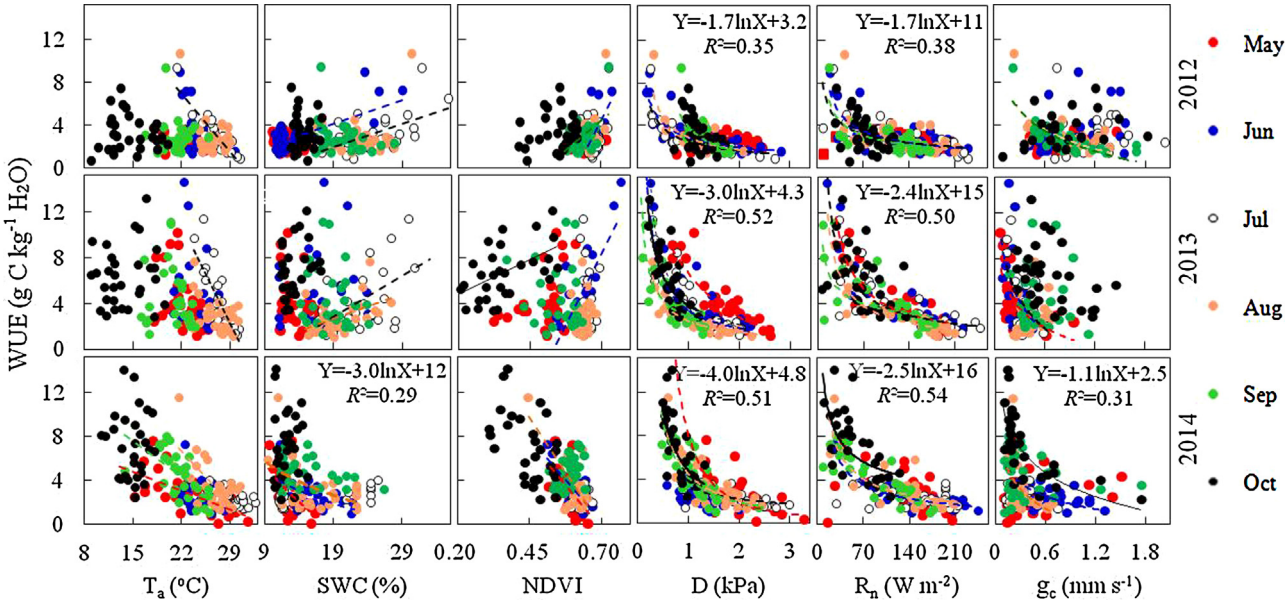

Fig. 4. Scatterplots of daily mean water use efficiency (WUE) and selected explanatory variables (*i.e.*, T_a, SWC, NDVI, D, R_n, and g_c) during the growing season (May–October) from 2012 to 2014 ($n = 80$, $p < 0.05$). Dashed lines provide logarithmic trends according to month. Vertical lines in plots for D, R_n, and g_c represent thresholds of logarithmic expressions.

Table 1
Annual mean water use efficiency (WUE, g C kg^{-1} H_2O), air temperature (T_a, °C), net radiation (R_n, W m^{-2}), vapor pressure deficit (D, kPa), and soil water content (SWC,%), annual total precipitation (P, mm), evapotranspiration (ET, mm), and gross ecosystem productivity (GEP, g C m^{-2}), and growing-season (from May to October) normalized difference vegetation index (NDVI) and growing-season length (GSL, days).

Year	WUE	T_a	R_n	D	SWC	P	ET	GEP	NDVI	GSL
2012	2.2	12.9	80	0.9	15.5	738	577	1295	0.64	197
2013	2.9	13.4	80	0.8	15.0	476	414	1196	0.55	183
2014	2.6	15.0	84	1.0	12.4	271	429	1094	0.60	192
Mean	2.6	13.8	81	0.9	14.3	495	473	1195	0.60	192
SD	0.2	0.6	1.3	0.1	0.9	135	52	58	0.08	4

length among the three years (Table 1; Fig. 1d, e). Daily and monthly WUE remained relatively constant in mid-summer (July–August) across all years (Figs. 1 f, 2 e). Unlike GEP and ET maximizing in summer, seasonal WUE reached its peak in autumn (Figs. 1 d, e, f, 2 e).

High g_c led to low WUE around noontime while the opposite was true in the morning. Hourly WUE followed a similar diurnal cycle across all years (Fig. 3), with the highest values in the early morning (*i.e.*, 8:00 Local Standard Time, LST) under conditions of increased T_a and R_n. On average, hourly WUE reached a maximum of 8 g C kg^{-1} H_2O in the morning. There was a secondary maxima in late afternoon (*i.e.*, 16:00–17:00 LST) in October under conditions of decreasing T_a and R_n for 2013 and 2014. Among the three years studied, mean hourly WUE was lowest in 2012.

3.3. Seasonal regulation of WUE

Within each season, interaction of daily NDVI and g_c (*i.e.*, $g_c \times$ NDVI) explained 38% of spring variation in WUE over the three years ($n = 277$; $p < 0.05$; Table 2). Daily interactions of $R_n \times T_a$ and $R_n \times$ D were more important in summer ($n = 277$; $p < 0.05$) and autumn ($n = 273$; $p < 0.05$), explaining 44% and 32% of seasonal variation in WUE, respectively (Table 2).

Daily WUE had a negative relationship with T_a across all years, particularly in July of 2012 and 2013, and May, August, and September of 2014. On average, daily WUE had negative relationships with D, R_n and g_c during the May-to-October period for all years (Fig. 4). A negative logarithmic function was able to describe the relationship between daily values of WUE and corresponding D, R_n and g_c fairly well. In general, daily WUE decreased radically as these factors increased, when D <1.1 kPa, R_n <70 W m^{-2}, or g_c <0.6 mm s^{-1} (Fig. 4).

Table 2
Pearson's correlation coefficient (*PCC*) between daily water use efficiency (WUE, g C kg^{-1} H_2O) and the most important regulatory variables (*RV*) during spring (March–May), summer (June–August), and autumn (September–November) of years 2011, 2012, and 2013; where n = 92 for each season. Tested variables included biophysical and environmental variables, *i.e.*, daily mean stomatal conductance (g_c, mm s^{-1}), air temperature (T_a, °C), net radiation (R_n, W m^{-2}), vapor pressure deficit (D, kPa), normalized difference vegetation index (NDVI) and soil water content (SWC, %), and total precipitation (P, mm).

		2012	2013	2014
Spring	*RV*	P	NDVI	g_c
	PCC	0.38	0.44	0.42
Summer	*RV*	g_c	T_a	R_n
	PCC	−0.42	−0.43	−0.47
Autumn	*RV*	NDVI	D	R_n
	PCC	−0.38	−0.39	−0.41

In contrast, daily WUE had a positive relationship with SWC and NDVI in June and/or July in 2012 and 2013 (Fig. 4). In contrast, daily WUE formed a negative relationship with SWC and NDVI in an excessively dry year (*i.e.*, 2014; Fig. 4), particularly in May, June, and August. On average, daily WUE decreased radically when SWC <16% in 2014, with a measured peak value of 14.1 g C kg^{-1} H_2O in 2014 (Fig. 4). On a monthly basis, WUE also had a negative relationship with T_a, NDVI, precipitation, and SWC across all years (Fig. 2), *i.e.*, WUE was lowest in summer, when values of the explanatory variables were high.

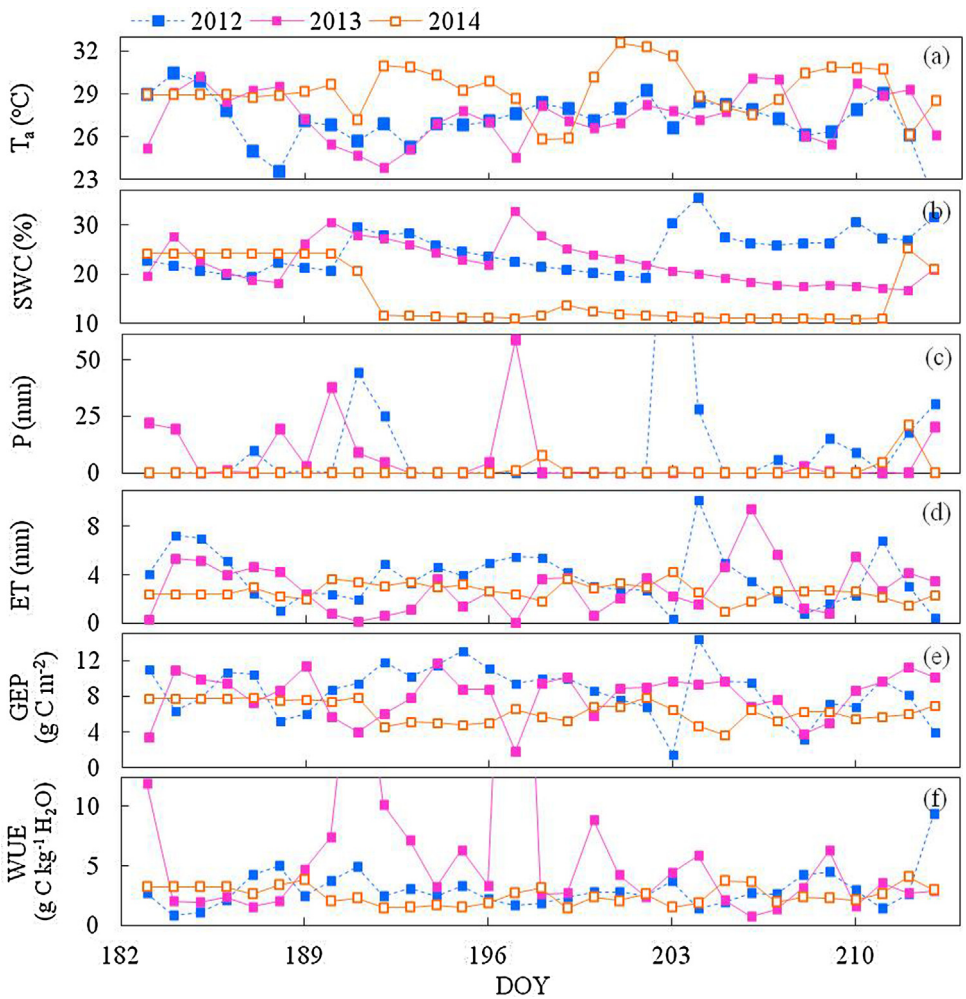

Fig. 5. Daily mean (a) T_a, (b) SWC, (c) total precipitation (P), (d) ET, (e) GEP, and (f) daily mean WUE for July of 2012–2014 (*i.e.*, DOY 182–213). One precipitation value (*i.e.*, on DOY 203 in 2012) and two WUE values (*i.e.*, on DOY 191 and DOY 197 both in 2013) are not completely shown as they are out of range compared to the majority of points shown.

3.4. Seasonal water availability in regulating WUE

Daily WUE decreased during dry days or remained nearly constant at low levels during extremely dry days over the growing season (Figs. 1 f, 5 f). An extreme dry-soil period in 2014 (DOY 191–210) caused GEP and WUE to remain low under high T_a and hyper-arid conditions, with a low mean SWC of 11% (Fig. 5). In addition, daily WUE decreased from 10.1 g C kg^{-1} H_2O on DOY 192–3.4 g C kg^{-1} H_2O on DOY 196 in 2013, with no precipitation and a decreasing SWC of 27.3–22.0% during this period. Similarly, on a monthly basis, WUE remained relatively constant from May to August of 2014, with high monthly T_a, low monthly SWC, and extremely low monthly precipitation (Fig. 2). Although July received the greatest quantity of precipitation, it was generally a dry month for both 2012 and 2013 and an extremely dry month for 2014, with 10 consecutive non-rainy days in July in 2012 (DOY 193–202), 10 days in 2013 (DOY 198–207), and 15 days in 2014 (DOY 183–197; Fig. 5c).

In contrast, daily WUE was higher on rainy days than on rain-free days ($p < 0.05$, based on a *t*-test; Figs. 1 f, 2). In general, a small increase in WUE was observed on rainy days, due to a larger decrease in ET than in GEP, with both GEP and ET increasing on the second day (Fig. 5). A slight increase in WUE occurred in both 2012 and 2013 during consecutive rainy days (DOY 183–197), with both ET and GEP increasing during this period (Fig. 5). Daily WUE increased during this period from 0.9 to 4.9 g C kg^{-1} H_2O in 2012 and 2.0–27.1 g C kg^{-1} H_2O in 2013, with total precipitation of 56 mm in 2012 and 89 mm in 2013 (Fig. 5). In addition, an extremely intense precipitation event on DOY 203, 2012, caused ET to decrease more than GEP on that day, resulting in an increase in WUE compared to its level during the preceding day (+1.2 g C kg^{-1} H_2O; Fig. 5). This extremely intense precipitation had a one-day lag effect, increasing ET more than GEP, resulting in a low daily WUE of 1.4C kg^{-1} H_2O with a high SWC of 35.7% on DOY 204, 2012 (Fig. 5).

4. Discussion

4.1. Comparison of annual WUE with other sites

Mean ecosystem WUE (GEP:ET; 2.2–2.9 g C kg^{-1} H_2O) for this protected urban forest fell within the reported annual ranges of 2.1–3.8 g C kg^{-1} H_2O for naturally-growing temperate conifer forests (Kuglitsch et al., 2008; Beer et al., 2009). Our mean annual WUE was also very close to the annual value reported for another forest plantation in the suburbs of Beijing (*i.e.*, 2.5 g C kg^{-1} H_2O; Xiao et al., 2013); while notwithstanding mean annual GEP, ET, and precipitation at our site were significantly lower than those reported at the other site, giving a mean difference of 239 g C m^{-2}, 113 mm, and 74 mm between sites. These differences suggest that relatively dry conditions at our site likely decreased both GEP

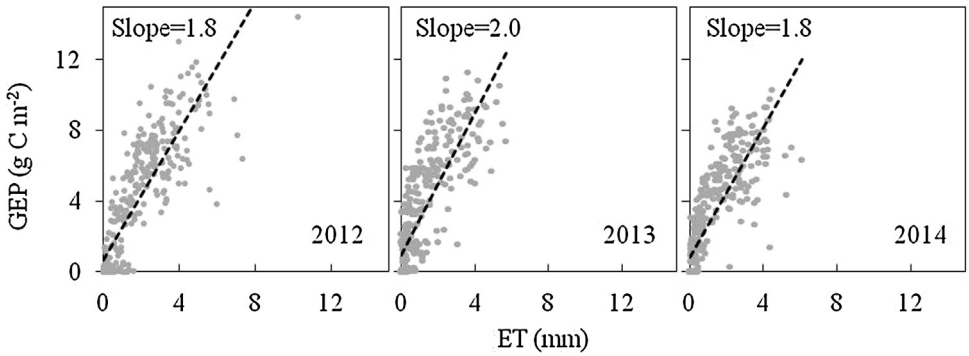

Fig. 6. Annual linear relationship between daily gross ecosystem production (GEP) and evapotranspiration (ET); black dashed lines give the fitted linear trend between GEP and ET for the three years ($n = 365$, $p < 0.0001$).

and ET proportionally; causing annual WUE to fall within those reported ranges.

Our study site is located in an urbanized area (*i.e.*, Beijing city) and the urban heat-island effect should have intensified as a result of contrasting responses of urban- and rural-surface energy budgets to intense heating (Li et al., 2015). Yet, impacts of urbanization at our site, including high CO_2 concentrations, were not significant on account of (a) Beijing's policy, which restricts human disturbance on protected parkland ecosystems in the middle of the northeastern section of the park; and (b) the large physical dimensions of the forest reserve, which potentially helped to offset a significant level of urban warming by stimulating greater ET and cooling of the area.

4.2. WUE response to seasonal drought and for different phenophases

The three-year study (2012–2014) provided a unique opportunity to study the seasonal and interannual responses of ecosystem WUE to extreme drought. Seasonal water availability combined with variable drought severity and duration during periods of changing T_a caused seasonal ET and GEP to respond differently, introducing significant departures in WUE to localized drought. Dry soils during leaf expansion and increasing T_a, led to a lower annual WUE in 2012 and 2014, compared to 2013 (Fig. 1a, f; Table 1), which was likely due to a larger reduction in GEP than in ET during leaf expansion (Fig. 1d, e). Additionally, extreme drought during leaf coloration (*i.e.*, in October), caused WUE to increase in 2013 and 2014, mainly as a result of drought and low T_a, SWC, and NDVI. This caused ET to decrease significantly more than GEP (Figs. 1, 2). In contrast, high monthly SWC during early spring to early summer (*i.e.*, from March to June; Figs. 1 a, 2 d) of 2013 likely caused the high growing-season WUE, compared to the WUE of the same time period in 2012 and 2014 (Fig. 1a, f; Table 1). We concluded that high SWC during the leaf-expansion period was more important than SWC in mid-summer or autumn for maintaining a high seasonal WUE (Figs. 1 a, f, 2 d, e), and thus, regulating interannual variation in WUE.

Extremely dry conditions, coupled with the highest annual T_a, caused annual WUE to be of moderate value due to proportional reductions in seasonal GEP and ET in 2014 (Table 1; Figs. 1, 2). In the extremely dry July of 2014, when T_a and R_n reached their individual maxima, water availability to the urban forest was substantially limited, resulting in extremely low SWC (Fig. 5a, b, f). Such summer warming and extreme drought potentially reduced both transpiration and photosynthetic capacity, resulting in inhibited plant growth as a result of self-protection by stomatal regulation against water losses (Fig. 3); in other words the stomata minimized the possibility of xylem cavitation and adjusted to maintain a sustainable flow of water (Kuglitsch et al., 2008; Niu et al., 2011). Consequently, monthly GEP and ET in July of 2014 were both lowest among the three years. Yet, GEP decreased more than ET, causing WUE to be low (Fig. 5d–f).

4.3. Biophysical controls on WUE evolution at multiple timescales

An advantage of WUE, which is estimated at the ecosystem-level, is that it essentially reflects a compromise between water loss and biomass gain. Ecosystem water and C fluxes were intimately linked (Fig. 6), since transpiration and photosynthesis C fixation are both affected by stomatal opening. The slope of the coupled ET and GEP was higher in 2013 and lower in 2012 and 2014 (Fig. 6), of which the annual trends observed were consistent with those of WUE appearing in Table 1. Additionally, we found that coupled daily ET and GEP was stronger than coupled daily ET and NEP on an annual basis. Since determination of NEP depends on ER, and ER is not strongly coupled to water fluxes, this may obscure the coupling of canopy water and C fluxes.

It has been found that biophysical controls of ET and GEP in a forest ecosystem were reflected in the form of g_c change, which controlled the response of WUE to seasonal drought (Zha et al., 2013). Hourly WUE was simultaneously regulated by g_c during the growing season (Fig. 3). Lower hourly g_c and WUE in the summer months of 2013 and 2014 are likely because of the partial closing of the stomata, which was in response to high summer T_a, R_n and D and low precipitation and SWC, jointly causing GEP to decrease more than ET partly due to metabolic limitations. There was a clear decrease in hourly WUE from 10:00 to 14:00 LST under conditions of increased T_a and R_n for both 2013 and 2014 (Fig. 3), which increased ET relatively more than GEP because of higher diffusivity of water vapor than CO_2 in air. Although g_c calculated from Eq. (4) does not explicitly represent the biophysical parameter of stomatal conductance, theoretical and experimental investigations have shown that g_c is often related to the weighted integration of individual leaves (Baldocchi and Meyers, 1998). Thus, g_c can be considered as a biological control on ecosystem WUE.

Ecosystem responses to environmental change are usually driven by the response of a dominant species at the site. Seasonal and interannual variation in WUE suggest that afforestation of urban-forest parks mainly mixed with *P. tabulaeformis,* provides a means of increasing C uptake with an acceptable investment in external water resources. We concluded that a short-term, off-season acute drought (*e.g.*, during the leaf-coloration period of 2013) failed to lead to a low autumn or annual WUE, likely as a result of not only abundant spring soil water but also drought-resistance characteristics of *P. tabulaeformis*. Yet, the negative impact of long-lasting droughts may cause water stress in urban forests to develop and further impede plant growth, resulting in a GEP decrease and

an associated decline in WUE. Negative relationships between daily WUE and T_a, D, R_n, and g_c during the growing season (Fig. 4) reflected that urban forests consisting of *P. tabulaeformis* generally consume water more effectively at moderate levels of T_a, R_n, D, and g_c. Thus, moderate levels of available energy (through T_a and R_n) and D and g_c were sufficient to maintain a relatively high growing-season WUE. Since current measurements span over three years, a long-term study is needed to (i) assess the effects of extreme droughts at different phenophases on interannual variability in WUE; and to (ii) investigate the role that the urban heat-island effect may have on the interannual variability in an urban forest's WUE.

5. Conclusions

Patterns in ecosystem WUE of a protected urban forest were examined in light of combined influences of biological and extreme environmental variables. Moderate levels of available energy (through T_a and R_n), D and g_c were sufficient to maintain a relatively high growing-season WUE for this forest plantation. Seasonal and interannual variation in WUE suggests that afforestation of urban-forest park mainly mixed with *P. tabulaeformis*, which provides a means to increase C uptake with an acceptable investment in external water resources. Daily WUE was decreased by seasonal warming and drying. Seasonal WUE remained unaffected during an extreme drought in the summer due to proportional decreases in GEP and ET. We concluded that the magnitude of an urban forest's WUE was modified by differential responses in GEP and ET to seasonal water stress for different phenophases. A longer-term study is needed to evaluate the impact of extreme drought and the "urban heat-island effect" on interannual variability in an urban forest's WUE.

Acknowledgements

This research was supported by grants from National Natural Science Foundation of China (NSFC; 31361130340, 31270755), the Beijing Science and Technology Project (z141100006014031) China Postdoctoral Science Foundation funded project (2013M540055), and the Academy of Finland (Project No. 14921). This work is related to the ongoing Finnish-Chinese research collaboration project EXTREME, between the Beijing Forestry University (BJFU) and the University of Eastern Finland (UEF). The U.S.-China Carbon Consortium (USCCC) promoted this work via helpful discussions and the exchange of ideas. We thank Peng Liu and Cai Ren for their assistances with field measurements and instrumentation maintenances and Gabriela Shirkey for editing the language of the manuscript.

References

Acevedo, O.C., Moraes, O.L.L., Degrazia, G.A., Fitzjarrald, D.R., Manzi, A.O., Campos, J.G., 2009. Is friction velocity the most appropriate scale for correcting nocturnal carbon dioxide fluxes? Agric. For. Meteorol. 149, 1–10.

Baldocchi, D.D., Meyers, T.P., 1998. On using eco-physiological, micrometeorological and biogeochemical theory to evaluate carbon dioxide, water vapor and trace gas fluxes over vegetation: a perspective. Agric. For. Meteorol. 90, 1–25.

Beer, C., Ciais, P., Reichstein, M., Baldocchi, D., Law, B.E., Papale, D., Soussana, J.F., Ammann, C., Buchmann, N., Frank, D., Gianelle, D., Janssens, I.A., Knohl, A., Kostner, B., Moors, E., Roupsard, O., Verbeeck, H., Vesala, T., Williams, C.A., Wohlfahrt, G., 2009. Temporal and among-site variability of inherent water use efficiency at the ecosystem level. Glob. Biogeochem. Cycles, 23, http://dx.doi.org/10.1029/2008GB003233 (GB2018).

Bell, J.E., Weng, E., Luo, Y., 2010. Ecohydrological responses to multifactor global change in a tallgrass prairie: a modeling analysis. J. Geophys. Res. 115, G04042, http://dx.doi.org/10.1029/2009JG001120.

De Boeck, H.J., Lemmens, C.M.H.M., Bossuyt, H., Malchair, S., Carnol, M., Merckx, R., Nijs, I., Ceulemans, R., 2006. How do climate warming and plant species richness affect water use in experimental grasslands. Plant Soil 288, 249–261.

Falge, E., Baldocchi, D.D., Olson, R., Anthoni, P., Aubinet, M., Bernhofer, C., Burba, G., Ceulemans, R., Clement, R., Dolman, H., Granier, A., Gross, P., Grünwald, T., Hollinger, D., Jensen, N.O., Katul, G., Keronen, P., Kowalski, A., Lai, C.T., Law, B.E., Meyers, T., Moncrieff, J., Moors, E., Munger, J.W., Pilegaard, K., Rannik, Ü., Rebmann, C., Suyker, A., Tenhunen, J., Tu, K., Verma, S., Vesala, T., Wilson, K., Wofsy, S., 2001. Gap filling strategies for defensible annual sums of net ecosystem exchange. Agric. For. Meteorol. 107, 43–69.

Flanagan, L.B., Johnson, B.G., 2005. Interacting effects of temperature: soil moisture and plant biomass production on ecosystem respiration in a northern temperate grassland. Agric. For. Meteorol. 130, 237–253.

Gao, Y., Zhu, X., Yu, G., He, N., Wang, Q., Tian, J., 2014. Water use efficiency threshold for terrestrial ecosystem carbon sequestration in China under afforestation. Agric. For. Meteorol 195–196, 32–37.

Hmimina, G., Dufrene, E., Pontailler, J.-Y., Delpierre, N., Aubinet, M., Caquet, B., de Grandcour, A., Burban, B., Flechard, C., Granier, P., Gross, A., Heinesch, B., Longdoz, B., Moureaux, C., Ourcival, J.M., Rambal, S., Saint Andre, L., Soudani, K., 2013. Evaluation of the potential of MODIS satellite data to predict vegetation phenology in different biomes: an investigation using ground-based NDVI measurements. Remote Sens. Environ. 132, 145–158.

Hu, Z., Yu, G., Fu, Y., Sun, X., Li, Y., Shi, P., Wang, Y., Zheng, Z., 2008. Effects of vegetation control on ecosystem water use efficiency within and among four grassland ecosystems in China. Glob. Change Biol. 14, 1609–1619.

Huang, M., Piao, S., Sun, Y., Ciais, P., Cheng, L., Mao, J., Poulter, B., Shi, X., Zeng, Z., Wang, Y., 2015. Change in terrestrial ecosystem water-use efficiency over the last three decades. Glob. Change Biol., http://dx.doi.org/10.1111/gcb.12873.

Krishnan, P., Black, T.A., Grant, N.J., Barr, A.G., Hogg, E.T.H., Jassal, R.S., Morgenstern, K., 2006. Impact of changing soil moisture distribution on net ecosystem productivity of a boreal aspen forest during and following drought. Agric. For. Meteorol. 139, 208–223, http://dx.doi.org/10.1016/j.agrformet.2006.07.002.

Kuglitsch, F.G., Reichstein, M., Beer, C., Carrara, A., Ceulemans, R., Granier, A., Janssens, I.A., Koestner, B., Lindroth, A., Loustau, D., Matteucci, G., Montagnani, L., Moors, E.J., Papale, D., Pilegaard, K., Rambal, S., Rebmann, C., Schulze, E.D., Seufert, G., Verbeeck, H., Vesala, T., Aubinet, M., Bernhofer, C., Foken, T., Grünwald, T., Heinesch, B., Kutsch, W., Laurila, T., Longdoz, B., Miglietta, F., Sanz, M.J., Valentini, R., 2008. Characterisation of ecosystem water-use efficiency of European forests from eddy covariance measurement. Biogeosci. Dis. 5, 4481–4519.

Law, B.E., Falge, E., Gu, L., Baldocchi, D.D., Bakwin, P., Berbigier, P., Davis, K., Dolman, A.J., Falk, M., Fuentes, J.D., Goldstein, A., Granier, A., Grelle, A., Hollinger, D., Janssens, I.A., Jarvis, P., Jensen, N.O., Katul, G., Mahli, Y., Matteucci, G., Meryrs, T., Monson, R., Munger, W., Oechel, W., Olson, R., Pilegaard, K., Poaw, K.T., Thorgeirsson, H., Valentini, R., Verma, S., Vesala, T., Wilson, K., Wofsy, S., 2002. Environmental controls over carbon dioxide and water vapour exchange of terrestrial vegetation. Agric. For. Meteorol. 113, 97–120, http://dx.doi.org/10.1016/S0168-1923(02)00104-111.

Li, S., Eugster, W., Asanuma, J., Kotani, A., Davaa, G., Oyunbaatar, D., Sugita, M., 2008. Response of gross ecosystem productivity, light use efficiency, and water use efficiency of Mongolian steppe to seasonal variations in soil moisture. J. Geophys. Res. 113, G01019, http://dx.doi.org/10.1029/2006JG00349.

Li, D., Sun, T., Liu, M., Yang, L., Wang, L., Gao, Z., 2015. Contrasting responses of urban and rural surface energy budgets to heat waves explain synergies between urban heat islands and heat waves. Environ. Res. Lett. 10, 054009, http://dx.doi.org/10.1088/1748-9326/10/5/054009.

Massman, W.J., Lee, X., 2002. Eddy covariance flux corrections and uncertainties in long-term studies of carbon and energy exchanges. Agric. For. Meteorol. 113, 121–144.

Niu, S., Zhang, Z., Xia, J., Zhou, X., Song, B., Li, L., Wan, S., 2011. Water use efficiency in response to climate change—from leaf to ecosystem in a temperate steppe. Glob. Change Biol. 17, 1073–1082.

Noormets, A., Chen, J., Crow, T.R., 2007. Age-dependent changes in ecosystem carbon fluxes in managed forests in northern Wisconsin. U. S. A. Ecosyst. 10, 187–203.

Ponce-Campos, G.E., Moran, M.S., Huete, A., Zhang, Y., Bresloff, C., Huxman, T.E., Eamus, D., Bosch, D.D., Buda, A.R., Gunter, S.A., Scalley, T.H., Kitchen, S.G., McClaran, M.P., McNab, W.H., Montoya, D.S., Morgan, J.A., Peters, D.P.C., Sadler, E.J., Seyfried, M.S., Starks, P.J., 2013. Ecosystem resilience despite large-scale altered hydroclimatic conditions. Nature 494, 349–352.

Ponton, S., Flanagan, L.B., Alstad, K.P., Johnson, B.G., Morgenstern, K., Kljun, N., Black, T.A., Barr, A.G., 2006. Comparison of ecosystem water-use efficiency among Douglas-fir forest aspen forest and grassland using eddy covariance and carbon isotope techniques. Glob. Change Biol. 12, 294–310.

Reichstein, M., Ciais, P., Papale, P., Valentini, R., Running, S., Viovy, N., Cramer, W., Granier, A., Oge, J., Allard, V., Aubinet, M., Bernhofer, C., Buchmann, N., Carrara, A., Grünwald, T., Heimann, M., Heinesch, B., Knohl, A., Kutsch, W., Loustau, D., Manka, G., Matteucci, G., Miglietta, F., Ourcival, J.M., Pilegaard, K., Pumpanen, J., Rambal, S., Schaphoff, S., Seufert, G., Soussana, J.F., Sanz, M.J., Vesala, T., Zhao, M., 2007. Reduction of ecosystem productivity and respiration during the European summer 2003 climate anomaly: a joint flux tower, remote sensing and modelling analysis. Glob. Change Biol. 13, 634–651, http://dx.doi.org/10.1111/j.1365-2486.2006.01224.x.

Schmid, H.P., Grimmond, C.S.B., Cropley, F.D., Offerle, B., Su, H.B., 2000. Measurements of CO_2 and energy fluxes over a mixed hardwood forest in the Midwestern United States. Agric. For. Meteorol. 103, 355–373.

Schotanus, P., Nieuwstadt, F.T.M., De Bruin, H.A.R., 1983. Temperature measurement with a sonic anemometer and its application to heat and moisture fluxes. Boundary Layer Meteorol. 26, 81–93.

Tang, J., Bolstad, P.V., Ewers, B.E., Desai, A.R., Davis, K.J., Carey, E.V., 2006. J. Geophys. Res. 111, G02009, http://dx.doi.10.1029/2005JG000083.
Xiao, J., Sun, G., Chen, J., Chen, H., Chen, S., Dong, G., Gao, S., Guo, H., Guo, J., Han, S., Kato, T., Li, Y., Lin, G., Lu, W., Ma, M., McNulty, S., Shao, C., Wang, X., Xie, X., Zhang, X., Zhang, Z., Zhao, B., Zhou, G., Zhou, J., 2013. Carbon fluxes, evapotranspiration, and water use efficiency of terrestrial ecosystems in China. Agric. For. Meteorol. 182–183, 76–90.
Xie, J., Chen, J., Sun, G., Chu, H.S., Noormets, A., Ouyang, Z., John, R., Wan, S., Guan, W., 2014. Long-term variability and environmental control of the carbon cycle in an oak-dominated temperate forest. Forest Ecol. Manag. 313, 319–328, http://dx.doi.org/10.1016/j.foreco.2013.10.032.
Xie, J., Jia, X., He, G., Zhou, C., Yu, H., Bourque, C.P.A., Liu, H., Zha, T., 2015. Environmental control over seasonal variation in carbon fluxes of an urban temperate forest ecosystem. Landscape Urban Plan. http://dx.doi.org/10.1016/j.landurbplan.2015.04.011.
Yang, B., Pallardy, S.G., Meyers, T., Gu, L.H., Hanson, P.J., Wullschleger, S.D., Heuer, M., Hosman, K.P., Riggs, J.S., Sluss, D.W., 2010. Environmental controls on water use efficiency during severe drought in an Ozark Forest in Missouri USA. Glob. Change Biol. 16, 2252–2271 http://dx.doi.10.1111/j.1365-2486.2009.02138.x.
Yoshida, M., Ohta, T., Kotani, A., Maximov, T., 2010. Environmental factors controlling forest evapotranspiration and surface conductance on a multi-temporal scale in growing seasons of a Siberian larch forest. J. Hydrol. 395, 180–189.
Yu, G.R., Song, X., Wang, Q., Liu, Y., Guan, D., Yan, J., Sun, X., Zhang, L., Wen, X., 2008. Water-use efficiency of forest ecosystems in eastern China and its relations to climatic variables. New Phytol. 177, 927–937.
Zha, T., Xing, Z., Wang, K., Kellomäki, S., Barr, A.G., 2007. Total and component carbon fluxes of a Scots pine ecosystem from chamber measurements and eddy covariance. Ann. Bot. 99, 345–353.
Zha, T., Li, C., Kellomaki, S., Peltola, H., Wang, K., Zhang, Y., 2013. Controls of evapotranspiration and CO_2 fluxes from scots pine by surface conductance and abiotic factors. PLoS One 8, e69027 http://dx.doi.10.1371/journal.pone.0069027.
Zhai, J., Su, B., Krysanova, V., Vetter, T., Gao, C., Jiang, T., 2010. Spatial variation and trends in PDSI and SPI indices and their relation to streamflow in 10 large regions of China. J. Climate 23, 649–663 http://dx.doi.10.1175/2009JCLI2968.1.
Zhang, F.M., Ju, W.M., Shen, S.H., Wang, S.Q., Yu, G.R., Han, S.J., 2014. How recent climate change influence water use efficiency in East Asia. Theor. Appl. Climatol. 116, 359–370 http://dx.doi.10.1007/s00704-013-0949-2.